Title

Molecular Phenotypes of Acute Respiratory Distress Syndrome in the ROSE Trial Have Differential Outcomes and Gene Expression Patterns That Differ at Baseline and Longitudinally over Time.

Journal

American Journal of Respiratory and Critical Care Medicine, 209(7)

Authors

Sinha, Pratik
Neyton, Lucile
Sarma, Aartik
et al.

Publication Date

2024-04-01

DOI

10.1164/rccm.202308-1490OC

Peer reviewed

ORIGINAL ARTICLE

Molecular Phenotypes of Acute Respiratory Distress Syndrome in the ROSE Trial Have Differential Outcomes and Gene Expression Patterns That Differ at Baseline and Longitudinally over Time

Pratik Sinha[1], Lucile Neyton[2], Aartik Sarma[2], Nelson Wu[2], Chayse Jones[2], Hanjing Zhuo[2], Kathleen D. Liu[2,3], Estella Sanchez Guerrero[4], Rajani Ghale[2,4], Christina Love[4], Eran Mick[4,7], Kevin L. Delucchi[5], Charles R. Langelier[4,7], B. Taylor Thompson[8], Michael A. Matthay[2,6], Carolyn S. Calfee[2,6], and the NHLBI PETAL Network

[1]Division of Clinical and Translational Research, Division of Critical Care, Department of Anesthesia, Washington University School of Medicine, St. Louis, Missouri; [2]Division of Pulmonary, Critical Care, Allergy and Sleep Medicine, [3]Division of Nephrology, and [4]Division of Infectious Diseases, Department of Medicine, [5]Department of Psychiatry and Behavioral Sciences, and [6]Department of Anesthesia, University of California, San Francisco, San Francisco, California; [7]Chan Zuckerberg Biohub, San Francisco, California; and [8]Division of Pulmonary and Critical Care, Department of Medicine, Massachusetts General Hospital, Boston, Massachusetts

ORCID IDs: 0000-0003-1273-2228 (L.N.); 0000-0002-7299-808X (E.M.).

Abstract

Rationale: Two molecular phenotypes have been identified in acute respiratory distress syndrome (ARDS). In the ROSE (Reevaluation of Systemic Early Neuromuscular Blockade) trial of cisatracurium in moderate to severe ARDS, we addressed three unanswered questions: *1*) Do the same phenotypes emerge in a more severe ARDS cohort with earlier recruitment; *2*) Do phenotypes respond differently to neuromuscular blockade? and *3*) What biological pathways most differentiate inflammatory phenotypes?

Methods: We performed latent class analysis in ROSE using preenrollment clinical and protein biomarkers. In a subset of patients ($n = 134$), we sequenced whole-blood RNA using enrollment and Day 2 samples and performed differential gene expression and pathway analyses. Informed by the differential gene expression analysis, we measured additional plasma proteins and evaluated their abundance relative to gene expression amounts.

Measurements and Main Results: In ROSE, we identified the hypoinflammatory (60.4%) and hyperinflammatory (39.6%) phenotypes with similar biological and clinical characteristics as prior studies, including higher mortality at Day 90 for the hyperinflammatory phenotype (30.3% vs. 61.6%; $P < 0.0001$). We observed no treatment interaction between the phenotypes and randomized groups for mortality. The hyperinflammatory phenotype was enriched for genes associated with innate immune response, tissue remodeling, and zinc metabolism at Day 0 and collagen synthesis and neutrophil degranulation at Day 2. Longitudinal changes in gene expression patterns differed dependent on survivorship. For most highly expressed genes, we observed correlations with their corresponding plasma proteins' abundance. However, for the class-defining plasma proteins in the latent class analysis, no correlation was observed with their corresponding genes' expression.

Conclusions: The hyperinflammatory and hypoinflammatory phenotypes have different clinical, protein, and dynamic transcriptional characteristics. These findings support the clinical and biological potential of molecular phenotypes to advance precision care in ARDS.

Keywords: ARDS; molecular phenotypes; RNA sequencing

(Received in original form August 27, 2023; accepted in final form February 12, 2024)

Supported by NHLBI Division of Intramural Research grant HL140026 (C.S.C.), National Institute of General Medical Sciences grant GM142992 (P.S.).

Author Contributions: Conception and design: P.S., M.A.M., B.T.T., and C.S.C. Assays, analysis, and interpretation: P.S., L.N., A.S., N.W., C.J., H.Z., E.S.G., R.G., C.L., E.M., K.L.D., C.R.L., K.D.L., and C.S.C. Drafting the manuscript for important intellectual content: P.S., L.N., A.S., N.W., C.J., H.Z., E.S.G., R.G., C.L., E.M., K.L.D., K.D.L., C.R.L., M.A.M., B.T.T., and C.S.C.

Correspondence and requests for reprints should be addressed to Pratik Sinha, M.B. Ch.B., Ph.D. Department of Anesthesia, Washington University School of Medicine, 660 South Euclid Avenue, Campus Box 8054, St. Louis, MO 63110. E-mail: p.sinha@wustl.edu.

This article has a related editorial.

This article has an online supplement, which is accessible from this issue's table of contents at www.atsjournals.org.

Am J Respir Crit Care Med Vol 209, Iss 7, pp 816–828, Apr 1, 2024

Originally Published in Press as DOI: 10.1164/rccm.202308-1490OC on February 12, 2024
Internet address: www.atsjournals.org

At a Glance Commentary

Scientific Knowledge on the Subject: Two molecular phenotypes have been identified in all comers in ARDS. The phenotypes have divergent biological and clinical characteristics, with increased mortality in the hyperinflammatory phenotype. Whether these phenotypes are identifiable in patients with more severe ARDS recruited at an early time point, as observed in ROSE (Reevaluation of Systemic Early Neuromuscular Blockade), remains unknown. Finally, the phenotypes are derived using proteins and clinical variables, and differences in transcriptional profiles of the phenotypes are poorly understood.

What This Study Adds to the Field: In a secondary analysis of the ROSE trial, we identified two phenotypes with characteristics similar to the previously described molecular phenotypes. Compared with previous ARDS trials, the proportion of hyperinflammatory phenotype in ROSE was higher, as was mortality in each phenotype. The two phenotypes had distinct transcriptional profiles at baseline and Day 2, with the hyperinflammatory phenotype's gene expression patterns suggestive of innate immune activation and metabolic dysfunction. The hypoinflammatory phenotype was associated with adaptive immune and IFN responses. Notably, we observed limited correlation between highly abundant proteins and their corresponding genes' expression. These findings suggest that the timing and severity of identifying the phenotypes have important implications, and studying transcriptomics in the context of the phenotypes offers orthogonal biological information.

Heterogeneity within the acute respiratory distress syndrome (ARDS) has been implicated in the consistent failure of clinical trials of pharmacotherapies, explained in part by the syndrome's broad and nonspecific diagnostic criteria (1, 2). Responding to this problem, our group has applied latent class analysis (LCA) to protein biomarker and clinical data to identify two molecular phenotypes of ARDS, termed hypoinflammatory and hyperinflammatory (3). To date, we have identified these two phenotypes in nine cohorts spanning three decades, including five randomized controlled trials (RCTs), three adult observational cohorts, and a pediatric trial cohort, totaling almost 5,000 patients (4–10). These phenotypes have been externally reproduced in observational cohorts from the United States and Europe (11, 12).

The hyperinflammatory phenotype is characterized by elevated plasma proinflammatory biomarkers and lower protein C and bicarbonate. In prior NHLBI RCTs of ARDS, the hyperinflammatory phenotype was the minority class (26% in ALVEOLI [Assessment of Low Tidal Volume and Elevated End-Expiratory Volume to Obviate Lung Injury], 27% in FACCT [Fluids and Catheters Treatment Trial], and 37% in SAILS [Statins for Acutely Injured Lungs from Sepsis]), with 90-day mortality (46% in ALVEOLI, 45% in FACCT, and 38% in SAILS) approximately 20% higher than for the hypoinflammatory phenotype (4, 7, 9).

Importantly, the phenotypes also appear to respond differently to randomized interventions as diverse as positive end-expiratory pressure (4), fluid management (7), and simvastatin (5). Despite this progress, numerous questions remain unanswered, including *1*) whether the phenotypes would be identified in an RCT with earlier recruitment and enriched for more severe ARDS, *2*) whether the phenotypes respond differently to neuromuscular blockade, and *3*) what biological pathways most differentiate the phenotypes.

The NHLBI Prevention and Early Treatment of Acute Lung Injury Network's ROSE (Reevaluation of Systemic Early Neuromuscular Blockade) trial was a recently completed multicenter, unblinded RCT of moderate to severe ARDS (Pa_{O_2}:FI_{O_2} < 150 mm Hg at screening) that tested the efficacy of cisatracurium infusion versus usual care (13). Patients were recruited to the trial exceptionally early, with a median duration of enrollment only 7.6 hours after meeting enrollment criteria. No treatment benefits were observed with cisatracurium therapy. In the present study, we leveraged these unique inherent characteristics of ROSE to answer the outlined key knowledge gaps regarding molecular phenotypes. We applied LCA to test for phenotypes using baseline clinical data and protein biomarkers from ROSE. Furthermore, in a subset of patients randomly selected to best represent each phenotype, we studied whole-blood transcriptomes to deepen our understanding of the biological features of each phenotype, including dynamic changes over time, and the post-transcriptional protein correlates of the most differentially expressed genes.

Methods

Study Population

This study was planned before the ROSE trial started, with approval from the NHLBI and Prevention and Early Treatment of Acute Lung Injury steering committee, including the plan to conduct LCA and deep biological phenotyping. A full report of the trial has been previously published (13). Briefly, between January 2016 and April 2018, ROSE enrolled 1,006 patients with ARDS in the United States with Pa_{O_2}:FI_{O_2} ratios <150 mm Hg while receiving a positive end-expiratory pressure of at least 8 cm H_2O. Five hundred one patients were randomized to continuous cisatracurium infusion and 505 patients to usual care (13). The primary outcome was all-cause mortality at Day 90 in any health care facility before discharge home. The trial was stopped early because of futility, with mortality in the treatment arm (42.5%) similar to that in the control arm (42.8%) and higher than anticipated *a priori*.

LCA

We conducted LCA using procedures described in our prior work (8, 9, 14). Briefly, we used demographics, preenrollment vital signs, clinical laboratory values, and research protein biomarkers as class-defining variables (*see* Table E1 in the online supplement). We fit five LCA models comprising one to five classes. The optimally fitting model for the population was determined using a combination of the Bayesian information criterion, the Vuong-Lo-Mendell-Rubin test, entropy, and the sample sizes of the smallest classes (14). Individual class membership was assigned using the highest posterior probability generated by the optimal model. Full details of the LCA procedures are provided in the

online supplement. As a sensitivity analysis, we repeated the above-described LCA procedures excluding patients from whom plasma samples were not collected.

To determine concordance with the previously described molecular phenotypes of ARDS, we used validated parsimonious three-variable (IL-8, protein C, and serum bicarbonate) and four-variable (three-variable model plus vasopressor use) classifier models to generate probabilities for belonging to the hyperinflammatory phenotype for each patient (15).

RNA Sequencing and Analysis

In a subset of patients, we sequenced whole-blood RNA using biospecimens from enrollment (Day 0) and Day 2. For these measurements, we randomly selected 67 patients with each phenotype from the 793 patients with biospecimen availability. At the time of selection, informed by the findings of the LCA and heterogeneity of treatment effect analysis, we chose to evaluate differences in gene expression among patients strongly representative of the phenotypes rather than to investigate the effect of the randomized intervention on expression patterns. To ensure that patients were strongly representative of the phenotypes, we limited the random patient selection to those with probability of class membership >0.9. Details of the power calculation, RNA extraction, and sequencing methods are reported in the online supplement.

For the differential gene expression analysis, voom (https://rdrr.io/bioc/limma/man/voom.html)-transformed counts were analyzed using limma version 3.44.3 (https://bioconductor.org/packages/release/bioc/html/limma.html) and Dream (variancePartition version 1.27.2; https://rdrr.io/github/GabrielHoffman/variancePartition/man/dream-method.html). Cross-sectional models were fit using fixed-effects models adjusted for *z*-scaled age and sex. We performed differential gene expression analysis comparing several groups (*see* Table E2), including the two molecular phenotypes at enrollment and changes over time between Day 0 and Day 2 samples within each phenotype. In exploratory analyses, we tested for differences in longitudinal changes in expression amounts for single genes between phenotypes and between survivorship groups within each phenotype. For these longitudinal analyses, we fit mixed-effects models adjusted for a random effect for individual subjects, age, gender, and treatment group allocation. To evaluate longitudinal gene expression changes between phenotypes, we modeled the interaction of phenotype with time. For longitudinal gene expression changes between survivorship groups in each phenotype, we modeled the interaction of time and survivorship. We used the Benjamini-Hochberg correction for all analyses in which we conducted multiple hypothesis testing. As the emphasis of RNA sequencing analyses was on discovery, we used an adjusted *P* value threshold of 0.1 to identify differentially expressed genes. Differentially enriched pathways in the Reactome database were identified using fgsea (16, 17). More details of these analyses are available in the online supplement.

Biomarker Quantification

The rationale and procedures for biomarker quantification used in the LCA have been described previously and are briefly summarized in the online supplement (4, 5). In the subset of patients with RNA sequencing, we measured nine additional protein biomarkers that were encoded by or associated with the most differentially expressed genes and/or the pathways enriched on the basis of data from Day 0, using multiplexed assays: IFN-α, IFN-β, IFN-γ, IL-10, IL-15, IP-10 (IFN-γ–induced protein 10), lipocalin, PDL-1 (programmed death ligand 1), and MMP-8 (matrix metalloproteinase 8) (R&D Systems). The final list of quantified proteins was also informed by whether a commercially available kit was available.

Other Statistical Considerations

Data are presented as mean ± SD, median (interquartile range), or count (percentage), and we tested differences using either Student's *t* test, the Wilcoxon rank test, or the χ^2 test depending on the type and distribution of the data. We plotted Kaplan-Meier survival curves censored at Day 90 to compare survival between phenotypes. We constructed receiver operating characteristic curves and used the area under the curve to evaluate model performance. To test for heterogeneity of treatment effect, we built logistic regression models with Day 90 mortality as the dependent variable and phenotype, randomized group, and their interaction term as the independent variables. We used Spearman's correlation coefficient to evaluate the relationship of gene expression and protein abundance.

LCA was performed using Mplus (version 8.1; Muthén & Muthén). All other analyses were performed using R software (https://www.r-project.org/) in RStudio version 1.0.143 (https://www.rstudio.com/).

Results

LCA Identified Two Classes in ROSE

On the basis of fit statistics, we found that the two-class model was a significantly better fit than the one-class model ($P < 0.0001$). Subsequent increases in model complexity did not result in significantly improved model fit (*see* Table E3). Median probabilities of class membership were 1.0 (0.96–1) and 1.0 (0.93–1) for classes 1 and 2 respectively, indicating well-separated classes. The two-class model was also the optimal fit in a sensitivity analysis that excluded patients with plasma samples missing (*see* Table E4).

In the two-class model, classes 1 and 2 comprised 608 (60%) and 398 (40%) patients, respectively. Previously described parsimonious models had high performance metrics, with areas under the curve of 0.94 (confidence interval, 0.92–0.96) for the three-variable model and 0.95 (confidence interval, 0.94–0.96) for the four-variable model compared with class assignment by LCA. These findings indicate high concordance with the previously described ARDS phenotypes; thus, for the rest of this report, we refer to class 1 as the hypoinflammatory phenotype and class 2 as the hyperinflammatory phenotype.

Differences in baseline characteristics of the phenotypes are presented in Table E5, with continuous class-defining variables shown in Figure 1A. The hyperinflammatory phenotype was characterized by higher concentrations of sTNFR1, Ang-2, IL-8, and IL-6 and lower concentrations of bicarbonate, protein C, and platelets. Among the categorical class-defining variables, there was no difference in gender (female: hypoinflammatory 43% vs. hyperinflammatory 46%; $P = 0.33$) or age (hypoinflammatory 55 ± 16 yr vs. hyperinflammatory 57 ± 15 yr; $P = 0.26$) between the phenotypes. Conversely, vasopressor use was significantly more common in the hyperinflammatory phenotype (85% vs. 41%; $P < 0.0001$). Primary ARDS risk factors (Figure 1B) differed significantly between the phenotypes ($P < 0.0001$), with pneumonia more frequent in the hypoinflammatory phenotype and

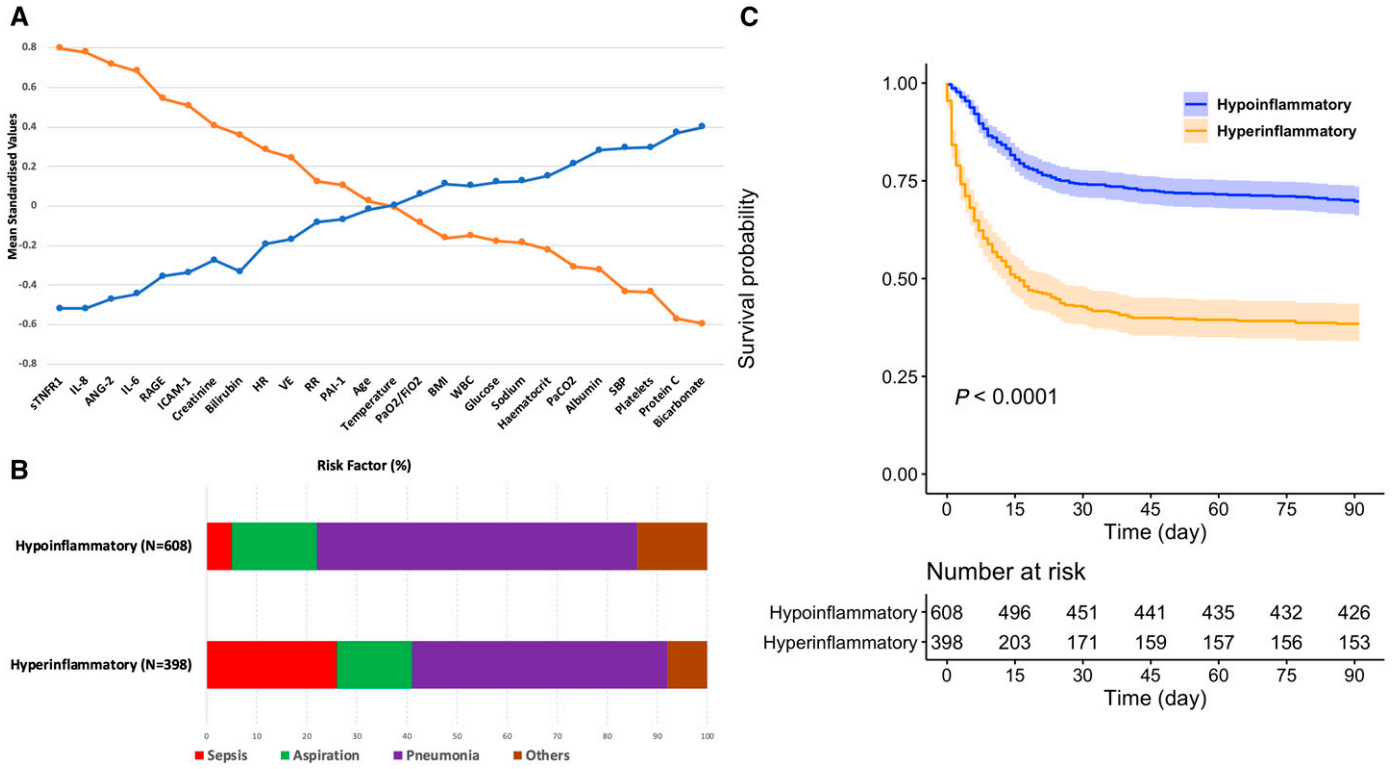

Figure 1. LCA using preenrollment data. (*A*) Comparison of class-defining variables between the two LCA-derived phenotypes. Standardized values for continuous class-defining variables used in the latent class models are shown. The variables are sorted from left to right in descending order for the highest values in the hyperinflammatory phenotype. Standardized values were calculated by assigning the mean of the variables as 0 and the SD as 1. (*B*) Differences in etiology between phenotypes. The proportion of patients with the major primary risk factors for acute respiratory distress syndrome in each phenotype is shown. (*C*) Survival curves comparing the two molecular phenotypes. Kaplan-Meier survival plots censored at Day 90 stratified by the two phenotypes are shown (the *P* value represents the Cox proportional-hazards test). ANG-2 = angiopoeitin-2; BMI = body mass index; HR = heart rate; ICAM-1 = intercellular adhesion molecule-1; LCA = latent class analysis; PAI-1 = plasminogen activator inhibitor-1; RAGE = receptor for advanced glycation products; RR = respiratory rate; SBP = systolic blood pressure; sTNFR1 = tumor necrosis factor receptor-1; VE = minute ventilation; WBC = white blood cell count.

sepsis more frequent in the hyperinflammatory phenotype.

The hyperinflammatory phenotype was associated with higher mortality and fewer ventilator-free days ($P < 0.0001$ for both; *see* Table E6). Notably, mortality in ROSE was higher for both the hypoinflammatory (30.3%) and hyperinflammatory (61.6%) phenotypes compared with analyses in prior NHLBI ARDS RCTs (4, 7, 9). Survival to Day 90 was significantly lower for the hyperinflammatory phenotype, with early separation of the curves observed from Day 1 onward (Figure 1C). In the hyperinflammatory phenotype, 34.2% of the deaths occurred by Day 2 and 61.2% by Day 7. In contrast, in the hypoinflammatory phenotype, only 7.6% of deaths occurred by Day 2 and 34.2% by Day 7. No significant treatment interaction was observed with the phenotypes and the randomized intervention ($P = 0.73$), with similar mortality at Day 90 within each phenotype when stratified by treatment group (Table 1).

Gene Expression Profiles in Molecular Phenotypes

After quality control steps, whole-blood sequencing data were available for 66 patients in the hypoinflammatory phenotype and 63 patients in the hyperinflammatory phenotype, with Day 0 data available in 63 and 60 patients, respectively (*see* Figure E1). The baseline characteristics of the two phenotypes in these randomly sampled subsets were similar to those of the whole cohort and are presented in Table E7.

Table 1. Mortality at Day 90 Stratified by the Molecular Phenotypes and Treatment Allocation

	Alive	Dead	Total	*P* Value
Hypoinflammatory				0.70
NMB	214 (69%)	96 (31%)	310	
Usual care	210 (70%)	88 (30%)	298	
Hyperinflammatory				0.91
NMB	74 (39%)	117 (61%)	191	
Usual care	79 (38%)	128 (62%)	207	

Definition of abbreviation: NMB = neuromuscular blockade.
P values are from chi-square tests.

At Day 0, 5,209 genes (26% of protein-coding genes) were significantly differentially expressed between the phenotypes (Figure 2A). Genes more highly expressed in the hyperinflammatory phenotype were associated with innate immune response (e.g., *OLFM4*, *CD177*, *S100A12*), tissue remodeling, and zinc metabolism (*see* Table E8). Genes more highly expressed in the hypoinflammatory phenotype were associated with vascular stability, transporters for antiinflammatory cytokines, and cell survival (*see* Table E8). A complete list of differentially expressed genes can be found in the online supplement. Pathway analysis showed that the hyperinflammatory phenotype was enriched for gene sets associated with cell cycling and death, metabolic and bioenergetics failure, and EIF2 (eukaryotic initiation factor 2) signaling (Figure 2B) pathways. The hypoinflammatory phenotype was enriched for pathways implicated in PD-1 (programmed cell death protein 1) and IFN signaling and glucocorticoid and mineralocorticoid synthesis (Figures 2B).

At Day 2, RNA sequencing data were available for 58 hypoinflammatory and 41 hyperinflammatory patients. Death between the time points was the cause for attrition in one patient in the hypoinflammatory phenotype and 14 patients in the hyperinflammatory phenotype. At Day 2, 3,279 genes were differentially expressed between the phenotypes (*see* Figure E2). On the basis of these differentially expressed gene sets, we observed pathways for collagen synthesis and breakdown and neutrophil degranulation enriched in the hyperinflammatory phenotype (Figure 3A). In contrast, pathways associated with PD-1 signaling and IFN signaling remained enriched on Day 2 in the hypoinflammatory phenotype. Pathway analyses generated using Ingenuity Pathway Analysis (Qiagen) database for differentially expressed gene sets between the phenotypes at Days 0 and 2 are presented in Figure E3.

The heatmap in Figure 3B depicts the genes with the greatest log fold changes between Day 0 and Day 2 in each phenotype. Genes that were most highly expressed at Day 0 (e.g., *RETN*, *MMP8*, and *LCN2*) in the hyperinflammatory phenotype were associated with the largest decreases in expression on Day 2; in contrast, genes with lower expression on Day 0, such as *MME*, *HAL*, and *ZNF608*, increased the most (Figure 3C).

In an exploratory analysis designed to better understand longitudinal transcriptional changes associated with survival in the hyperinflammatory phenotype, we evaluated the change in gene expression from Day 0 to Day 2 among 21 hyperinflammatory participants who survived to Day 90. Among survivors in the hyperinflammatory phenotype, the most differentially expressed genes between Days 0 and 2 (*see* Figure E4A) were enriched for pathways associated with defensins, antimicrobial peptides, and adaptive immune responses (*see* Figure E4B). In genes with the largest change between Days 0 and 2 in the hyperinflammatory phenotype (e.g., *MME*), we observed significant changes in expression amounts in survivors but not in nonsurvivors at the single-gene level (Figure 3D). Interestingly, on Day 2, average expression amounts of genes such as *ANGPT1*, *HAS1*, *KCNH3*, and *CYP27A1* converged according to survivorship rather than phenotype allocation (Figure 3D).

Next, informed by genes that were most differentially expressed between phenotypes at Day 0, we measured nine proteins in plasma samples obtained simultaneously (at preenrollment) in 63 patients in the hypoinflammatory phenotype and 59 patients in the hyperinflammatory phenotype. We excluded IFN-α, IFN-β, and IFN-γ from the analyses because of high proportions of measurements below the

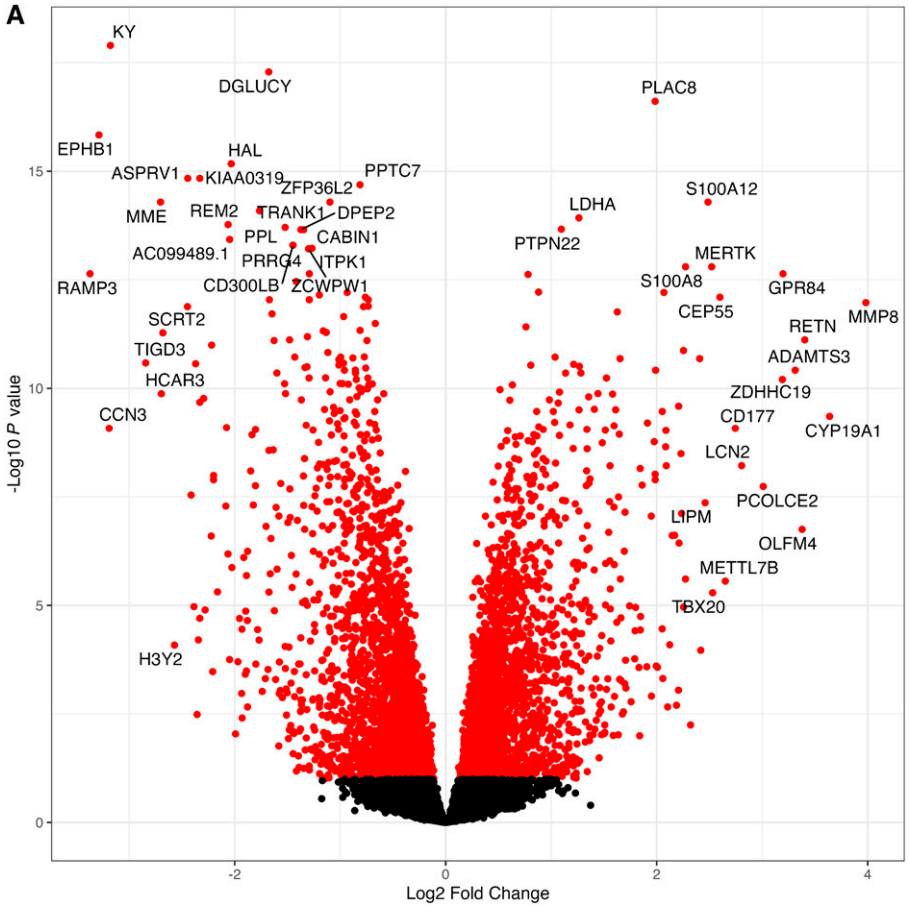

Figure 2. Gene expression analysis at Day 0. (*A*) DGE analysis between the hypoinflammatory and hyperinflammatory phenotypes. Volcano plot shows DGE analysis of whole-blood RNA sequencing data between the hypoinflammatory (left; $n = 63$) and hyperinflammatory (right; $n = 60$) phenotypes. Each point represents a gene (mRNA), and red dots represent genes with adjusted P values <0.1. Annotated genes represent the top 25 by either log fold change or the lowest P values. (*B*) Enriched gene sets in the two inflammatory phenotypes. NESs in gene sets are shown, on the basis of differentially expressed genes between the hyperinflammatory (orange) and hypoinflammatory (blue) phenotypes using the Reactome database.
DGE = differential gene expression; MMP8 = matrix metalloproteinase 8; NES = normalized enrichment score; Pd 1 = programmed cell death protein 1.

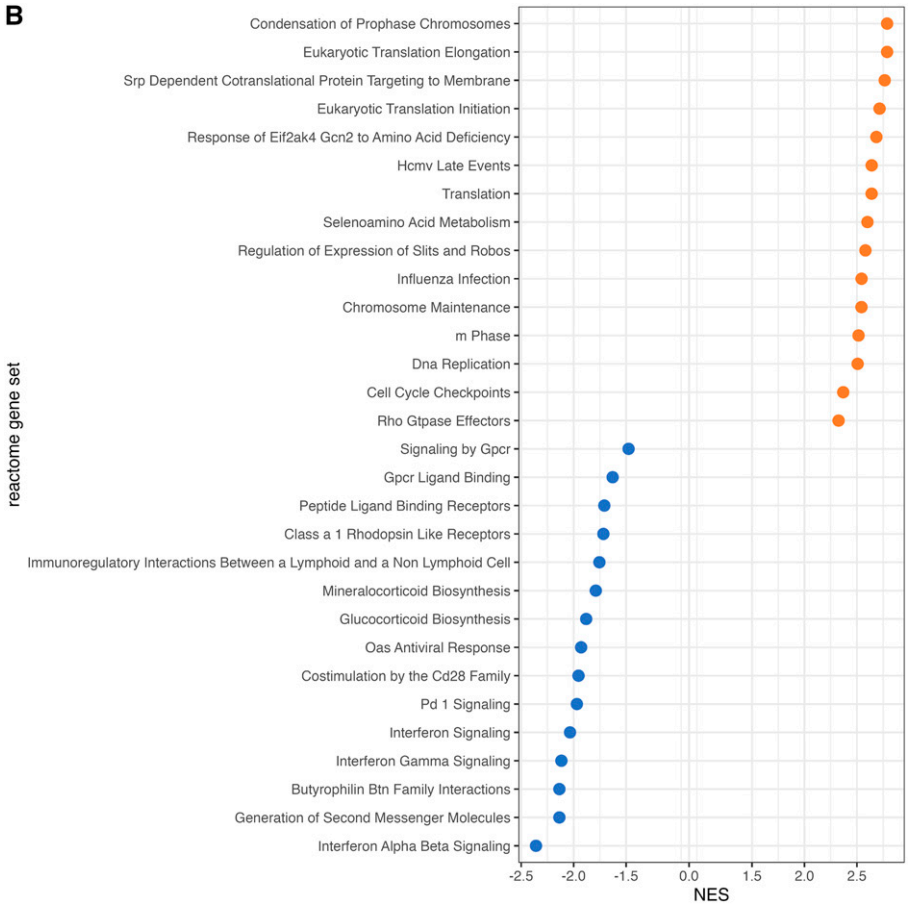

Figure 2. (*Continued*).

lower limit of detection (40–90%). Protein abundance for each phenotype is presented in Figure 4A. We observed that plasma protein concentrations of MMP-8, lipocalin, and IL-10 were higher in the hyperinflammatory phenotype and consistent with differences in gene expression patterns. In contrast, plasma protein concentrations of IL-15, PDL-1, and IP-10 were also higher in the hyperinflammatory phenotype, but the corresponding genes were more highly expressed in the hypoinflammatory phenotype (*see* Figure E5). Furthermore, we observed significant correlation between gene expression and quantified proteins for MMP-8, lipocalin, and IL-10 but not for IL-15 and PDL-1 (Figure 4B).

Given the observed discrepancies between genes' expression and their corresponding proteins' transcription, we evaluated the association between abundance of class-defining proteins and their corresponding genes' expression. As anticipated, in this subset, plasma proteins sTNFR1, IL-8, Ang-2, IL-6, ICAM-1, and RAGE were significantly higher in the hyperinflammatory phenotype (*see* Figure E6). However, corresponding gene expression patterns for these analytes followed different patterns, with gene expression either similar between phenotypes or lower in the hyperinflammatory phenotype (Figure 4C). Specifically, genes encoding for sTNFR1 and RAGE were significantly higher in the hypoinflammatory phenotype. Among the class-defining proteins, only sTNFR1 and RAGE were significantly correlated with their genes, but both were inversely correlated (*see* Figure E7).

Discussion

In ROSE, an RCT with earlier recruitment and more severe ARDS than prior RCTs in which we have performed LCA, we once again identified classes with clinical and biological characteristics strongly concordant with the previously described hypoinflammatory and hyperinflammatory phenotypes. The clinical implications of the phenotypes, however, differed from those of prior RCTs. Both the proportion of patients in the hyperinflammatory phenotype (40%) and the mortality in each phenotype were higher than previous RCTs. Notably, the mortality in the hyperinflammatory phenotype was 61%, with the majority of deaths occurring by Day 7 and a high proportion in the first 48 hours after enrollment. Taken together, these findings suggest that earlier measurement of protein biomarkers and phenotype classification may identify a large at-risk group for early mortality. These findings were consistent with findings from a prior observational ARDS cohort in which patient recruitment and sample acquisition were similarly early (8). We hypothesize that the higher and earlier mortality in ROSE may be attributed, in part, to the early enrollment of patients with more severe ARDS, which may have captured patients who would have otherwise been excluded because of severity or early death in prior ARDS RCTs.

The higher proportion of the hyperinflammatory phenotype with higher and early mortality in ROSE compared with prior NHLBI trials is likely due to the earlier recruitment and severity enrichment that was unique to ROSE. These findings suggest that the severity and timing of ARDS clearly matter when seeking phenotypes and have important implications for phenotyping using the recent global definition of ARDS, which proposes to extend the definition through inclusion of non–mechanically ventilated patients on high-flow nasal oxygen (18). The capture of patients at earlier time points and less severe ARDS will probably affect both the proportion of the phenotypes and their outcomes and/or may enable the discovery of novel phenotypes. For these reasons, the broadening of the ARDS definition is likely to be beneficial in understanding early and evolving phenotypes of ARDS.

We observed no differential treatment response to cisatracurium in the phenotypes. Although we can only speculate as to the reasons behind this observation, one likely explanation is that the treatment lacks efficacy in either phenotype. Alternatively, neuromuscular blockade might benefit the hyperinflammatory phenotype by facilitating

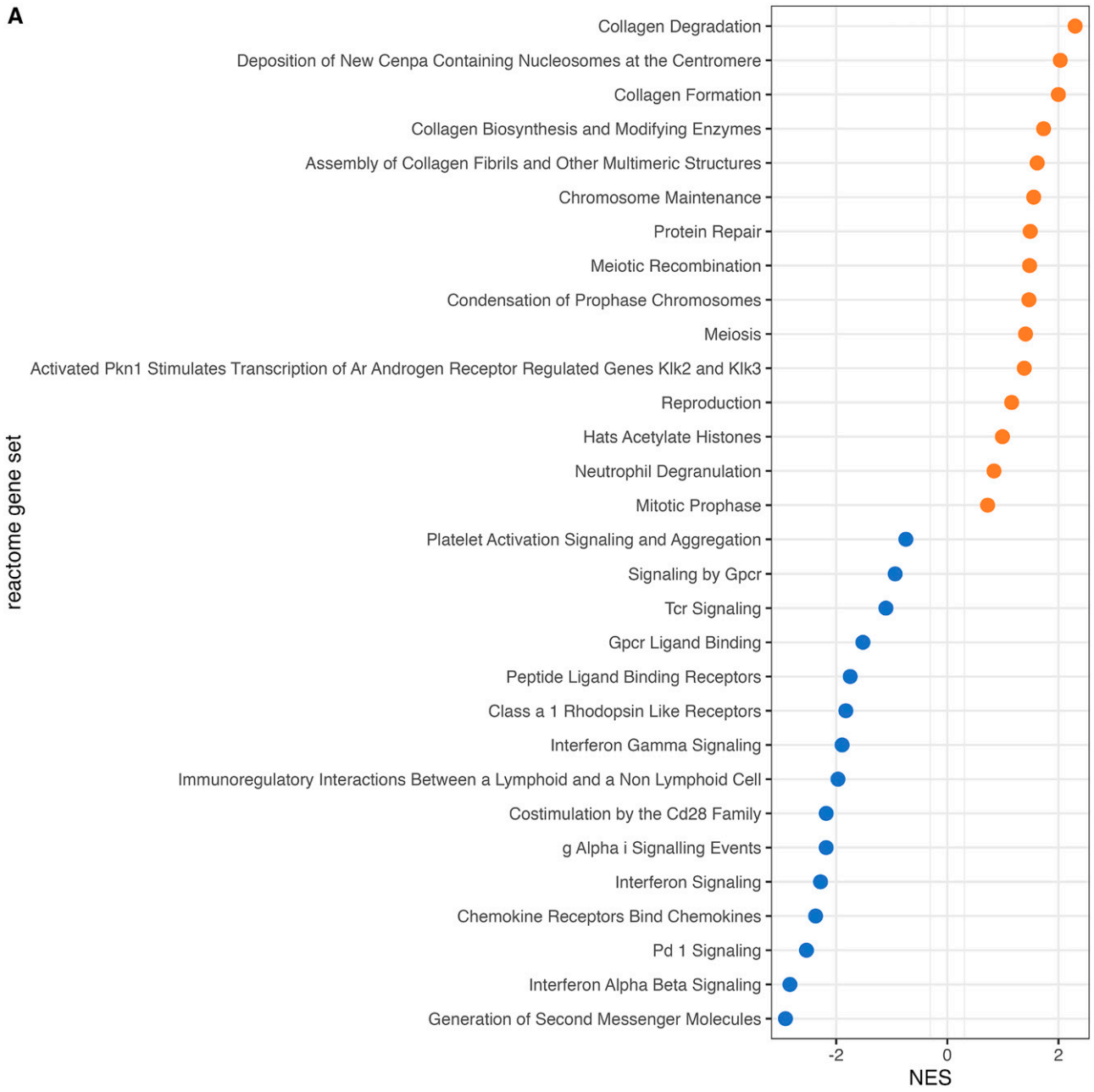

Figure 3. Time-dependent changes in gene expression comparing Day 2 with Day 0. (*A*) Gene sets enriched at Day 2 in the hypoinflammatory (Hypo) and hyperinflammatory (Hyper) phenotypes. Differences in NES in gene sets enriched on the basis of magnitudes of changes in gene expression patterns between Day 0 and Day 2 are shown for the Hyper (orange) and Hypo (blue) phenotypes. (*B*) Heatmap of top genes with significant phenotype-specific time changes between Day 0 and Day 2 in the Hypo and Hyper phenotypes. Gene expression patterns of the top 25 genes with phenotype-specific time profiles are shown. Red-colored values represent genes for which the expression increased between Day 0 and Day 2, and blue-colored values represent genes for which the expression decreased between Day 0 and Day 2. Thin bars at the top of the figure show findings of unsupervised clustering using hierarchical clustering. The two horizonal bars framing the top heatmap show the distribution of the inflammatory phenotypes and survivors and nonsurvivors in relation to the hierarchical clusters. (*C*) Changes in the expression of individual genes between Day 0 and Day 2 in the Hypo and Hyper phenotypes. Changes in average gene expression (transformed using variance-stabilizing transformation [VST]) in selected individual genes between Day 0 and Day 2 are shown with confidence intervals (***adjusted $P < 0.001$). (*D*) Changes in expression of individual genes between Day 0 and Day 2 stratified by molecular phenotypes and outcome. Changes in average expression (gene expression values transformed using VST) in selected individual genes between Day 0 and Day 2 are shown for survivors and nonsurvivors of each phenotype (***adjusted $P < 0.001$; significant P values were observed only among survivors in the Hyper phenotype, and all tests were nonsignificant in the Hypo phenotype survivorship groups and the Hyper nonsurvivors). MMP8 = matrix metalloproteinase 8; NES = normalized enrichment score; non-surv = nonsurvivors; NS = not significant; Pd 1 = programmed cell death protein 1; surv = survivors.

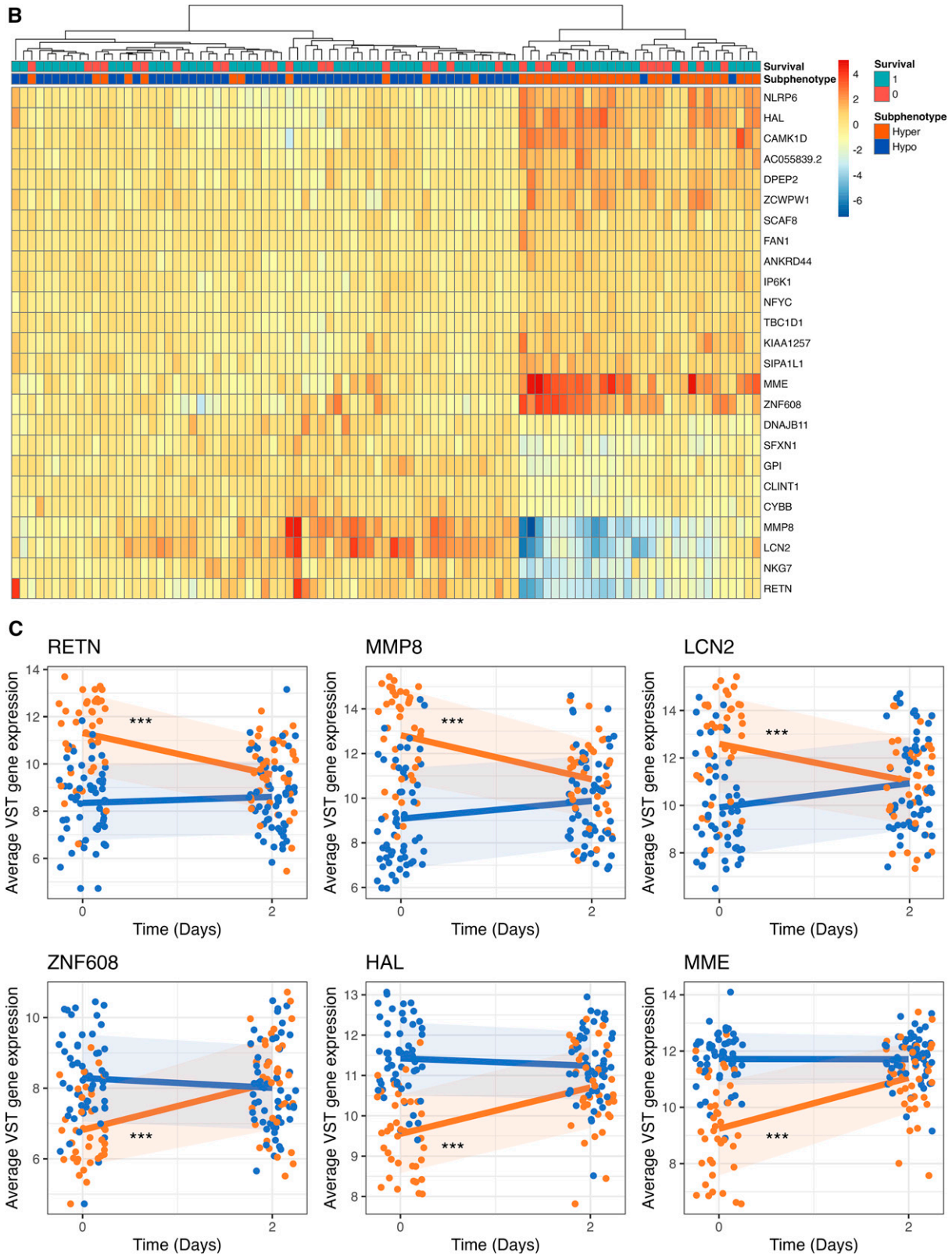

Figure 3. (*Continued*).

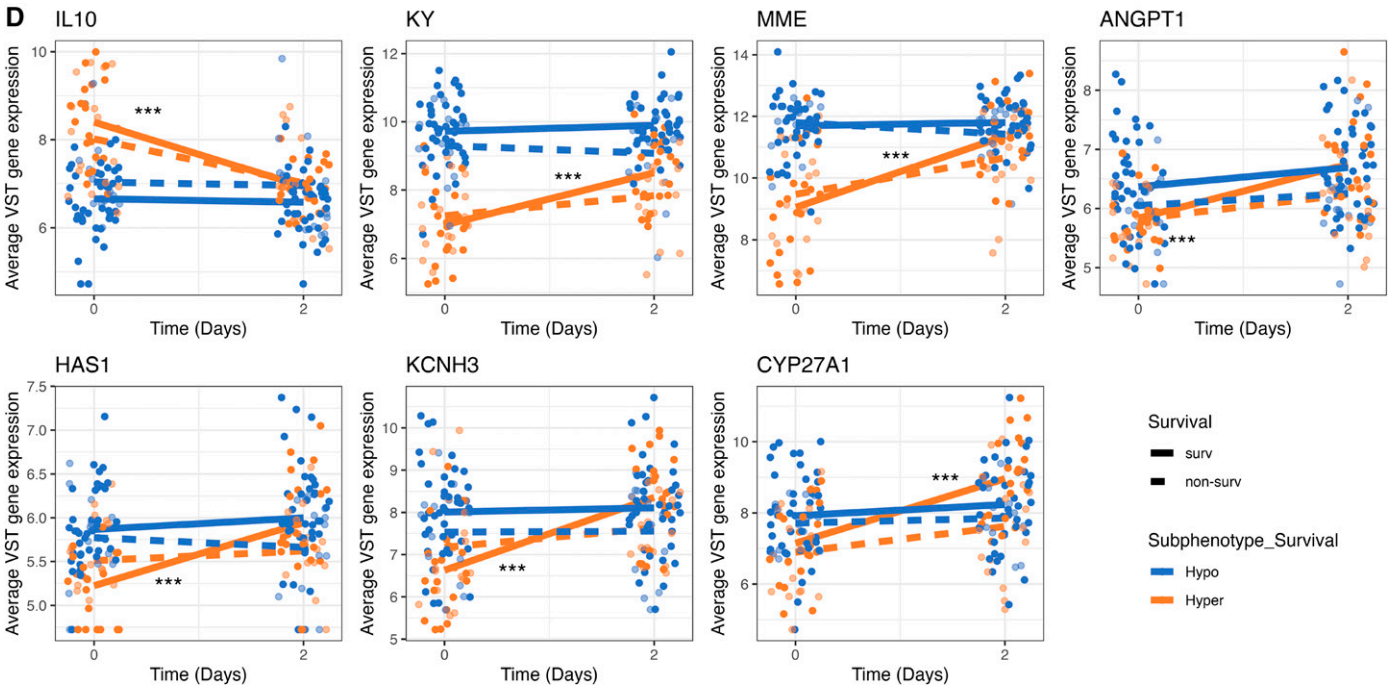

Figure 3. (*Continued*).

lung-protective ventilation, in which case we would expect the benefits to play out over several days rather than hours. The number of early deaths in the hyperinflammatory phenotype might then limit the power to detect efficacy of neuromuscular blockade in this phenotype. We did not have access to which patients in the usual care arm crossed over to receive neuromuscular blockade, which may have also potentially affected our treatment interaction analysis.

The analyses of whole-blood transcriptional data provided several important observations. First, the pathways enriched in each phenotype at Day 0 differed significantly. The hypoinflammatory phenotype was characterized by a transcriptional profile of IFN signaling and host viral responses, suggesting either a greater prominence of viral etiology or more robust antiviral response or both. In contrast, the transcriptomic pathways enriched in the hyperinflammatory phenotype at Day 0 were genes related to neutrophil activation, oxidative phosphorylation, and mitochondrial dysfunction. These findings are consistent with findings from Heijnen and colleagues, who used microarray data from blood leukocytes to study differences in molecular phenotypes in mechanically ventilated patients without ARDS (11). In another study, the same group of investigators sought to examine gene expression differences between their reactive and uninflamed phenotypes of ARDS, defined by plasma protein biomarkers only (19). In that study, the most differentially expressed genes in the reactive phenotype were remarkably similar to those observed in the hyperinflammatory phenotype (e.g., *MMP8*, *OLFM4*, and *RETN*), suggesting high overlap at a transcriptional level between these phenotyping schemas. In our view, these findings provide external face validity to the gene expression observations in our study. The association with mitochondrial dysfunction in the hyperinflammatory phenotype in these studies and ours also fits well with recent metabolomic data from our group (20).

A second novel observation from our transcriptional analyses related to changes in gene expression over time. Interestingly, by Day 2, gene sets associated with collagen synthesis and homeostasis increased the most in the hyperinflammatory phenotype, suggesting ongoing injury and aberrant repair signaling. These findings implicate the extracellular matrix as a potential site of ongoing injury in the hyperinflammatory phenotype. Whether these gene expression changes observed in whole blood mirror pathophysiology in the lungs remains unanswered and will require contemporaneous gene expression studies from the distal airspaces and blood.

A third important hypothesis-generating finding of our study was the longitudinal changes in gene expression between survivors and nonsurvivors, particularly the finding that expression amounts of some genes at Day 2 converged according to survivorship rather phenotypes. Increased expression of *ANGPT1*, which encodes for angiopoietin-1, and *HAS1*, which encodes for hyaluronan synthase 1, an enzyme associated with hyaluronic acid production, between Days 0 and 2 were most associated with survival in the hyperinflammatory phenotype. On Day 0, we observed lower expression of both genes; by Day 2 however, gene expression increased in survivors but remained low among nonsurvivors. For example, Ang-2, which is elevated in the hyperinflammatory phenotype, is an antagonist ligand to Ang-1 at the Tie-2 receptor, leading to endothelial dysfunction (21, 22). Binding of Ang-1 leads to vascular stabilization, and its potential as a therapeutic intervention has been

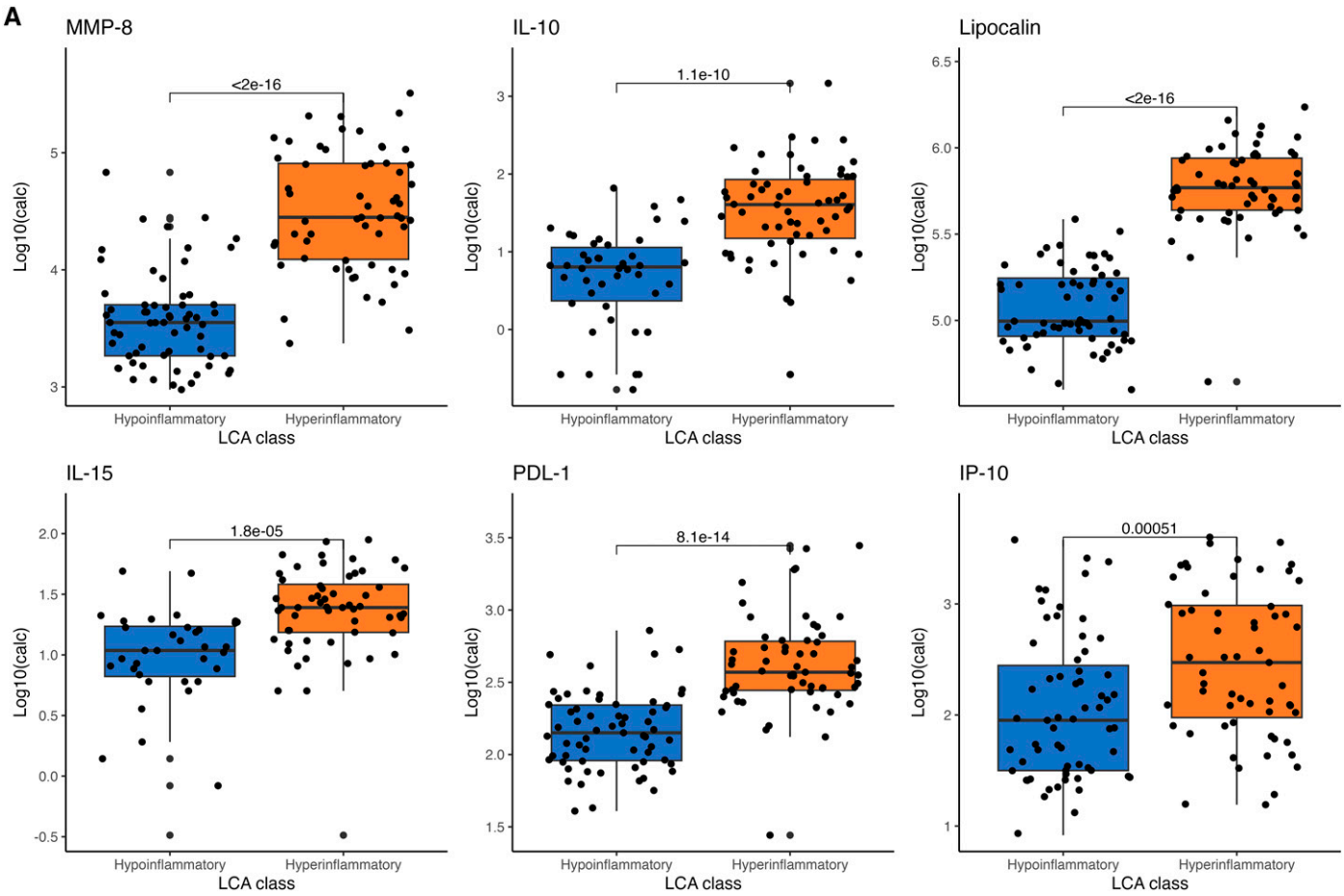

Figure 4. Comparison of gene expression and corresponding protein abundance. (*A*) Differences in concentrations of proteins corresponding to the most differentially expressed genes between the hypoinflammatory and hyperinflammatory phenotypes. (*B*) Correlation between gene expression amounts and protein concentrations in the two phenotypes of the most differentially expressed genes. (*C*) Differences in gene expression amounts of the mRNA transcripts of the class-defining proteins used in the LCA between the hypoinflammatory and hyperinflammatory phenotypes. AGER = receptor for advanced glycation end products; ANGPT2 = angiopoetin-2; calc = calculated from concentration of pg/mL; CXCL8 = IL-8; ICAM1 = intercellular adhesion molecule 1; IP-10 = IFN-γ–induced protein 10; LCA = latent class analysis; MMP-8 = matrix metalloproteinase 8; PDL-1 = programmed death ligand 1; R = overall Spearman's correlation coefficient; TNFRSF1A = tumor necrosis factor receptor 1; VST = variance-stabilizing transformation.

investigated in preclinical studies in sepsis (23, 24), ARDS (25), and pneumonia (26), and it may be of therapeutic value for the hyperinflammatory phenotype. It should be noted that our study design was not powered to detect differences in longitudinal gene expression between survivorship groups within the phenotypes. Therefore, these findings should be interpreted cautiously and need validation in larger samples sizes.

Although it is not known to what extent individual organs and tissue beds contribute to the observed plasma proteome in ARDS, we did observe significant positive correlation between mRNA expression and corresponding plasma protein concentrations for the genes that were most differentially expressed between the phenotypes, suggesting that RNA sequencing may be useful in identifying novel proteins to further discriminate or differentiate the phenotypes. In contrast, it is notable that most class-defining proteins did not correlate with their corresponding genes. Potential causes for this discrepancy include post-transcriptional factors, differences in protein clearance, and differing sources of circulating proteins versus transcripts (e.g., organs including the lung, liver, and kidney for proteins vs. circulating leukocytes alone for the transcripts). As a specific example, RAGE is highly expressed in the lung in ARDS, so high plasma concentrations of the sRAGE protein may originate from a pulmonary source, with the gene being less highly expressed in transcripts from circulating leukocytes.

Recently we have also identified these same two molecular phenotypes in multiple critically ill cohorts of sepsis patients (27). As several phenotypes have been described in sepsis using transcriptional data (28–30), the discordance in our data between plasma protein concentrations and corresponding gene transcripts raises important questions

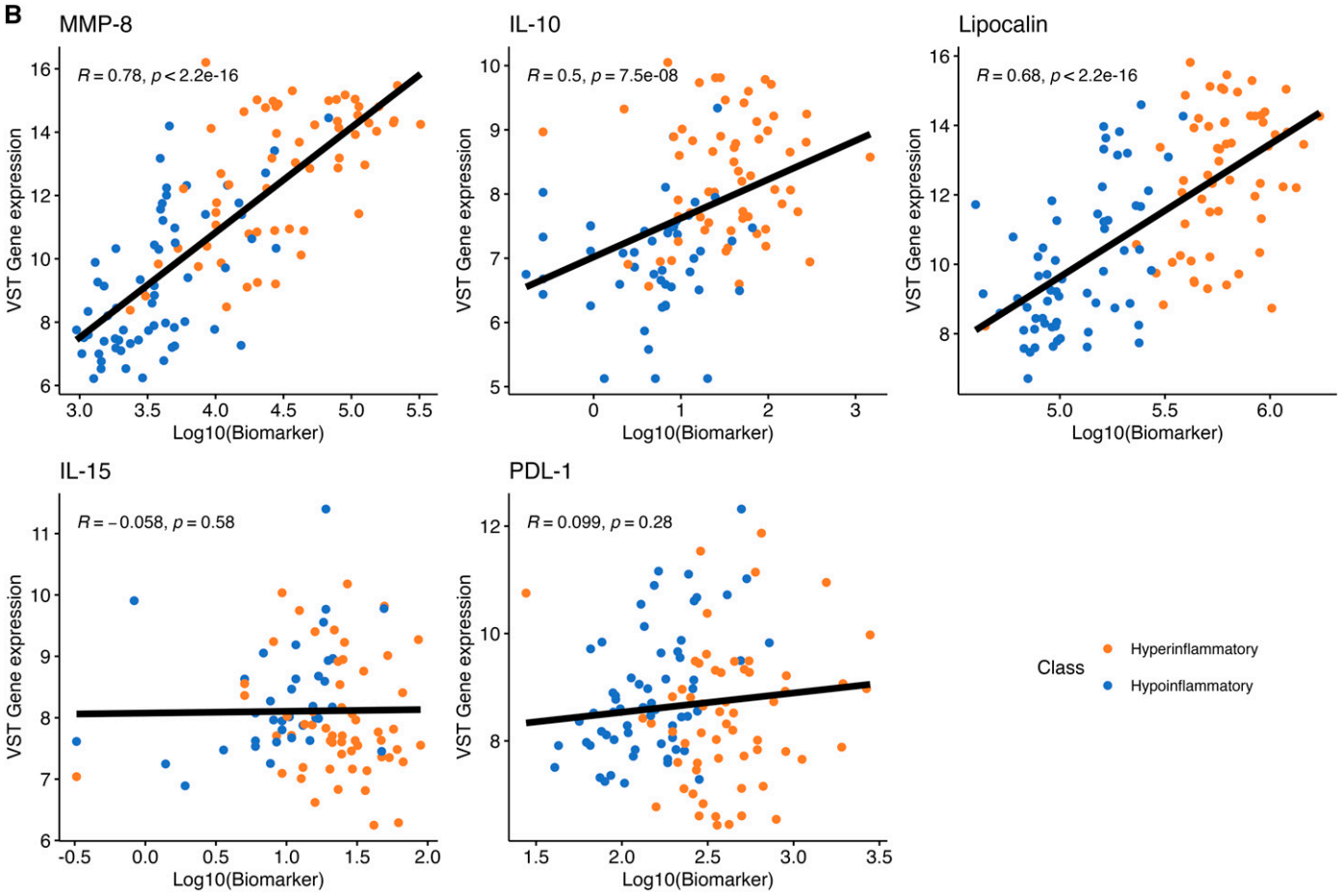

Figure 4. (*Continued*).

regarding the overlap of transcriptionally derived and molecularly derived phenotypes. Our data suggest that transcriptomics-based and protein biomarker–based approaches probably identify biologically distinct phenotypes with modest overlap. To this end, in a large observational cohort of patients with sepsis, investigators have recently shown that overlap between transcriptionally derived and the hypo- and hyperinflammatory phenotypes was low (31). Taken together, these findings suggest that phenotyping using transcriptomics and phenotyping using plasma proteins may be complementary when seeking to deliver precision-based care in critical illness.

Our study has several strengths, including its large sample size, which allowed testing for heterogeneity of treatment effect. The focus on a novel patient population (i.e., patients enrolled very early in the course of ARDS) as well as comprehensive quantification of protein biomarkers and the longitudinal RNA sequencing data are also important strengths.

The study also has some limitations. Although within this study we present no external validation of the LCA, the numerous independent replications we have previously published support the validity of the analyses (4, 5, 7, 8, 10). Given the cost of RNA sequencing, our sample size for the transcriptional analyses was limited to a subset of extremes of the two phenotypes. Although we adjusted our longitudinal analyses for confounders such as demographics and treatment group, we could not adjust for other factors that may potentially influence gene expression during the two time points, such as injurious ventilatory patterns and/or immunomodulators. Total white cell counts were similar between the phenotypes in the RNA sequencing subset; however, differential counts were not available, and we could not adjust for cell-specific differences between the phenotypes. Furthermore, we were unable to quantify protein biomarkers and evaluate their association with gene expression in longitudinal samples. The evaluation of the temporal kinetics of the phenotypes remains a key knowledge gap in the field. In a prior study, we reported that the statistical latent classes were stable over time (32); however, the stability of the biological features of the phenotypes remains poorly understood and represents an important future direction of research.

Conclusions

We report that the previously described hyperinflammatory and hypoinflammatory

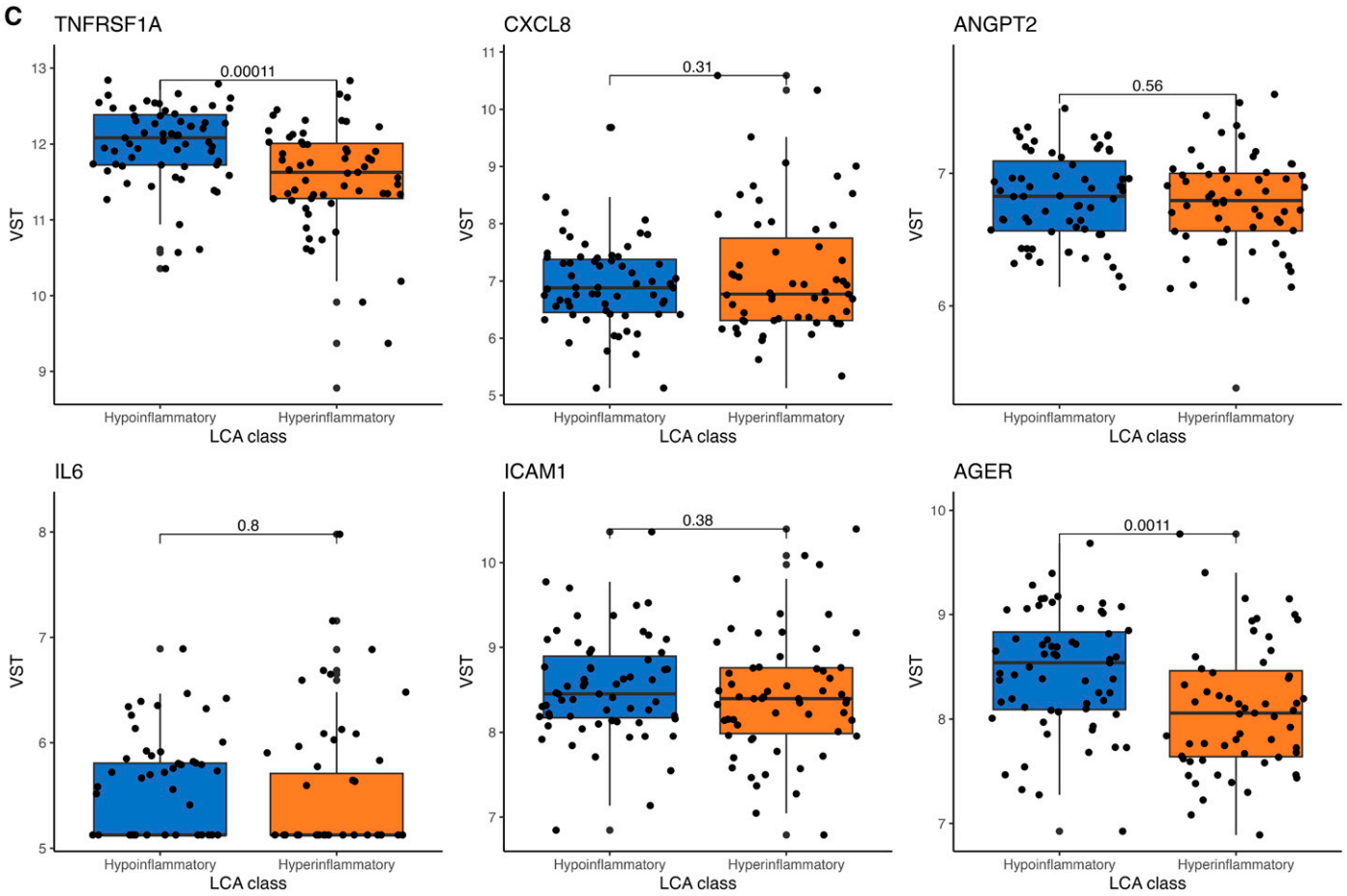

Figure 4. (*Continued*).

ARDS phenotypes are also observed in early, moderate to severe ARDS. Transcriptional profiling of the phenotypes reveals divergent biological signatures, where the hyperinflammatory signal is characterized by genes reflecting the innate immune response and the hypoinflammatory phenotype by IFN signaling. Longitudinal transcriptional changes within phenotypes were also informative, indicating differential signatures between survivors and nonsurvivors. As the field seeks to implement precision-based care, our findings provide further evidence that a phenotype-specific approach to studying biology can lead to the elucidation of potential pathways for therapeutic intervention. ■

Author disclosures are available with the text of this article at www.atsjournals.org.

References

1. Sinha P, Bos LD. Pathophysiology of the acute respiratory distress syndrome: insights from clinical studies. *Crit Care Clin* 2021;37: 795–815.
2. Matthay MA, McAuley DF, Ware LB. Clinical trials in acute respiratory distress syndrome: challenges and opportunities. *Lancet Respir Med* 2017;5:524–534.
3. Sinha P, Calfee CS. Phenotypes in acute respiratory distress syndrome: moving towards precision medicine. *Curr Opin Crit Care* 2019;25:12–20.
4. Calfee CS, Delucchi K, Parsons PE, Thompson BT, Ware LB, Matthay MA; NHLBI ARDS Network. Subphenotypes in acute respiratory distress syndrome: latent class analysis of data from two randomised controlled trials. *Lancet Respir Med* 2014;2:611–620.
5. Calfee CS, Delucchi KL, Sinha P, Matthay MA, Hackett J, Shankar-Hari M, *et al.*; Irish Critical Care Trials Group. Acute respiratory distress syndrome subphenotypes and differential response to simvastatin: secondary analysis of a randomised controlled trial. *Lancet Respir Med* 2018;6:691–698.
6. Dahmer MK, Yang G, Zhang M, Quasney MW, Sapru A, Weeks HM, *et al.*; RESTORE and BALI study investigators; Pediatric Acute Lung Injury and Sepsis Investigators (PALISI) Network. Identification of phenotypes in paediatric patients with acute respiratory distress syndrome: a latent class analysis. *Lancet Respir Med* 2022;10:289–297.
7. Famous KR, Delucchi K, Ware LB, Kangelaris KN, Liu KD, Thompson BT, *et al.*; ARDS Network. Acute Respiratory distress syndrome subphenotypes respond differently to randomized fluid management strategy. *Am J Respir Crit Care Med* 2017;195:331–338.

8. Sinha P, Delucchi KL, Chen Y, Zhuo H, Abbott J, Wang C, *et al.* Latent class analysis-derived subphenotypes are generalisable to observational cohorts of acute respiratory distress syndrome: a prospective study. *Thorax* 2022;77:13–21.
9. Sinha P, Delucchi KL, Thompson BT, McAuley DF, Matthay MA, Calfee CS; NHLBI ARDS Network. Latent class analysis of ARDS subphenotypes: a secondary analysis of the statins for acutely injured lungs from sepsis (SAILS) study. *Intensive Care Med* 2018;44:1859–1869.
10. Sinha P, Furfaro D, Cummings MJ, Abrams D, Delucchi K, Maddali MV, *et al.* Latent class analysis reveals COVID-19-related acute respiratory distress syndrome subgroups with differential responses to corticosteroids. *Am J Respir Crit Care Med* 2021;204:1274–1285.
11. Heijnen NFL, Hagens LA, Smit MR, Cremer OL, Ong DSY, van der Poll T, *et al.* Biological subphenotypes of acute respiratory distress syndrome show prognostic enrichment in mechanically ventilated patients without acute respiratory distress syndrome. *Am J Respir Crit Care Med* 2021;203:1503–1511.
12. Kitsios GD, Yang L, Manatakis DV, Nouraie M, Evankovich J, Bain W, *et al.* Host-response subphenotypes offer prognostic enrichment in patients with or at risk for acute respiratory distress syndrome. *Crit Care Med* 2019;47:1724–1734.
13. National Heart, Lung, and Blood Institute PETAL Clinical Trials Network; Moss M, Huang DT, Brower RG, Ferguson ND, Ginde AA, Gong MN, *et al.* Early neuromuscular blockade in the acute respiratory distress syndrome. *N Engl J Med* 2019;380:1997–2008.
14. Sinha P, Calfee CS, Delucchi KL. Practitioner's guide to latent class analysis: methodological considerations and common pitfalls. *Crit Care Med* 2021;49:e63–e79.
15. Sinha P, Delucchi KL, McAuley DF, O'Kane CM, Matthay MA, Calfee CS. Development and validation of parsimonious algorithms to classify acute respiratory distress syndrome phenotypes: a secondary analysis of randomised controlled trials. *Lancet Respir Med* 2020;8:247–257.
16. Gillespie M, Jassal B, Stephan R, Milacic M, Rothfels K, Senff-Ribeiro A, *et al.* The reactome pathway knowledgebase 2022. *Nucleic Acids Res* 2022;50:D687–D692.
17. Korotkevich G, Sukhov V, Budin N, Shpak B, Artyomov MN, Sergushichev A. Fast gene set enrichment analysis [preprint]. bioRxiv; 2021 [accessed 2023 Aug]. Available from: https://www.biorxiv.org/content/10.1101/060012v3.
18. Matthay MA, Arabi Y, Arroliga AC, Bernard G, Bersten AD, Brochard LJ, *et al.* A new global definition of acute respiratory distress syndrome. *Am J Respir Crit Care Med* 2024;209:37–47.
19. Bos LDJ, Scicluna BP, Ong DSY, Cremer O, van der Poll T, Schultz MJ. Understanding heterogeneity in biologic phenotypes of acute respiratory distress syndrome by leukocyte expression profiles. *Am J Respir Crit Care Med* 2019;200:42–50.
20. Alipanah-Lechner N, Neyton L, Mick E, Willmore A, Leligdowicz A, Contrepois K, *et al.* Plasma metabolic profiling implicates dysregulated lipid metabolism and glycolytic shift in hyperinflammatory ARDS. *Am J Physiol Lung Cell Mol Physiol* 2023;324:L297–L306.
21. Maisonpierre PC, Suri C, Jones PF, Bartunkova S, Wiegand SJ, Radziejewski C, *et al.* Angiopoietin-2, a natural antagonist for Tie2 that disrupts in vivo angiogenesis. *Science* 1997;277:55–60.
22. Augustin HG, Koh GY, Thurston G, Alitalo K. Control of vascular morphogenesis and homeostasis through the angiopoietin-Tie system. *Nat Rev Mol Cell Biol* 2009;10:165–177.
23. Kim DH, Jung YJ, Lee AS, Lee S, Kang KP, Lee TH, *et al.* COMP-angiopoietin-1 decreases lipopolysaccharide-induced acute kidney injury. *Kidney Int* 2009;76:1180–1191.
24. Witzenbichler B, Westermann D, Knueppel S, Schultheiss HP, Tschope C. Protective role of angiopoietin-1 in endotoxic shock. *Circulation* 2005;111:97–105.
25. McCarter SD, Mei SH, Lai PF, Zhang QW, Parker CH, Suen RS, *et al.* Cell-based angiopoietin-1 gene therapy for acute lung injury. *Am J Respir Crit Care Med* 2007;175:1014–1026.
26. Gutbier B, Neuhauß AK, Reppe K, Ehrler C, Santel A, Kaufmann J, *et al.*; CAPNETZ and PROGRESS Study Groups. Prognostic and pathogenic role of angiopoietin-1 and -2 in pneumonia. *Am J Respir Crit Care Med* 2018;198:220–231.
27. Sinha P, Kerchberger VE, Willmore A, Chambers J, Zhuo H, Abbott J, *et al.* Identifying molecular phenotypes in sepsis: an analysis of two prospective observational cohorts and secondary analysis of two randomised controlled trials. *Lancet Respir Med* 2023;11:965–974.
28. Burnham KL, Davenport EE, Radhakrishnan J, Humburg P, Gordon AC, Hutton P, *et al.* Shared and distinct aspects of the sepsis transcriptomic response to fecal peritonitis and pneumonia. *Am J Respir Crit Care Med* 2017;196:328–339.
29. Davenport EE, Burnham KL, Radhakrishnan J, Humburg P, Hutton P, Mills TC, *et al.* Genomic landscape of the individual host response and outcomes in sepsis: a prospective cohort study. *Lancet Respir Med* 2016;4:259–271.
30. Scicluna BP, van Vught LA, Zwinderman AH, Wiewel MA, Davenport EE, Burnham KL, *et al.*; MARS consortium. Classification of patients with sepsis according to blood genomic endotype: a prospective cohort study. *Lancet Respir Med* 2017;5:816–826.
31. van Amstel RBE, Cremer OL, van Vught LA, Bos LDJ; MARS Consortium. Subphenotypes in critical illness: a priori biological rationale is key. *Intensive Care Med* 2024;50:299–301.
32. Delucchi K, Famous KR, Ware LB, Parsons PE, Thompson BT, Calfee CS; ARDS Network. Stability of ARDS subphenotypes over time in two randomised controlled trials. *Thorax* 2018;73:439–445.